J. Quant. Spectrosc. Radiat. Transfer Vol. 28, No. 3, pp. 199–212, 1982
Printed in Great Britain.

0022-4073/82/090199-14$03.00/0

CALCULATION OF MEAN COLLISION CROSS SECTIONS OF FREE RADICAL OH WITH FOREIGN GASES

AHMED KHAYAR and JEANINE BONAMY
Laboratoire de Physique Moléculaire, ERA No. 834, Faculté des Sciences et des Techniques, La Bouloie, Route de Gray, 25030 Besancon Cedex, France

(*Received* 16 *November* 1981)

Abstract—The mean collision cross sections of OH perturbed by foreign gases have been calculated for microwave and far infrared spectra in the $X^2\Pi$ electronic ground state. A semi-classical formalism is used, which includes a parabolic description of the trajectory. The interaction potential is described as a sum of electrostatic contributions and both short-range and long-range anisotropic forces by using an atom–atom potential model. Good quantitative agreement is obtained between calculated and experimental linewidths.

1. INTRODUCTION

The OH radical has been the subject of extensive studies because it plays a significant role in the mesosphere and high stratosphere. Moreover, experiments[1,2] have demonstrated microwave resonance absorption by this free radical. To make future searches more fruitful, many laboratory investigations were performed which have yielded very accurate results for electronic ground state transitions up to the 9th vibrational level.[3] However, there are only a few[4–7] experimental determinations of the pressure broadening of rotational or microwave lines of OH, while very few calculations of line broadening parameters were performed.[8] There are two reasons for this deficiency. Because the free radical concentrations are very low, an experimental set-up with great sensivity is needed; also, free radicals are produced by chemical reactions and are highly diluted in complex gas mixtures. Thus, broadening of free radical lines in the absorption cell is caused by all perturbers present, the relative proportions of which are not accurately known.

Our purpose is to calculate line broadening by foreign gases of the microwave and rotational lines of OH in a semi-classical formalism[9] for a realistic intermolecular potential.

2. THEORY

The present formalism was developed[9] with the aim of treating diatom–diatom collisions, for which more involved treatments are not yet available. Several assumptions are made about the nature of the collisions. The colliding particles are assumed to follow classical bent trajectories and the collisions are binary. The theory is based on the impact approximation, which states that the duration of a collision is short compared with the time between collisions. Our treatment can be applied only for moderate gas densities which depend on the nature of the foreign gas. Starting from Eqs. (2)–(11) of Ref. 9, the expression for the half line width at half intensity of a pure rotational or microwave $f \leftarrow i$ transition is

$$\gamma_{fi}(\mathrm{cm}^{-1}) = \frac{n_b}{2\pi c}\,\bar{v}\sigma_{fi}$$

$$= \frac{n_b}{2\pi c}\sum_{J_2}\rho_{J_2}\int_0^\infty v f(v)\,\mathrm{d}v\int_0^\infty 2\pi b\,\mathrm{d}b\{1-[1-S^{(L)}_{2,f2i2}]$$

$$\times\exp[-(S_{2,f2}+S_{2,i2}+S^{(C)}_{2,f2i2})]\cos[S'_{2,f2}-S'_{2,i2}]\}, \qquad (1)$$

where n_b is the numerical density of the perturbing gas, c the speed of light, $f(v)$ the Maxwell–Boltzmann distribution of relative velocities. In practice, the velocity average is approximated by replacing v by $\bar{v}$, where $\bar{v}$ is the Maxwell–Boltzmann average collision velocity. The quantity σ_{fi} is the optical collision cross section summed over all occupied rotational states of the perturbing molecule with Boltzmann factor ρ_{J_2}. An integration is also

performed over the impact parameter b. The second order S_2 contributions are defined for diatomic molecules through

$$S_{2,f2i2}^{(C)} = \sum_{J_2'} S_{2,f2'i2'}\delta_{J_2'J_2},$$

$$S_{2,f2i2}^{(L)} = \sum_{J_2'} S_{2,f2'i2'}(1-\delta_{J_2'J_2}), \tag{2}$$

where

$$S_{2,f2'i2'} = -\frac{\hbar^{-2}}{(2J_i+1)(2J_2+1)} \sum_{\substack{M_f,M_f',M_i,M_i' \\ M_2,M_2'}} C(J_fJJ_i;\ M_f, M, M_i)$$

$$\times C(J_fJJ_i;\ M_f', M, M_i') \int_{-\infty}^{+\infty} \mathrm{d}t\ \mathrm{e}^{i\omega_{J_2'J_2}t} \langle J_fM_f'J_2'M_2'|\, V_{\mathrm{ANISO}}[r(t)]|J_fM_fJ_2M_2\rangle$$

$$\times \int_{-\infty}^{+\infty} \mathrm{d}t'\, \mathrm{e}^{i\omega_{J_2J_2'}t'} \langle J_iM_iJ_2M_2|\, V_{\mathrm{ANISO}}[r(t')]|J_iM_i'J_2'M_2'\rangle \tag{3}$$

and

$$S_{2,i2} = \frac{\hbar^{-2}}{2} \frac{1}{(2J_i+1)(2J_2+1)} \sum_{\substack{J_f',M_i' \\ J_2',M_2' \\ M_f,M_2}} \left| \int_{-\infty}^{+\infty} e^{i\omega_{J_fJ_2,J_f'J_2'}t} \right. \tag{4}$$

$$\left. \times \langle J_iM_iJ_2M_2|\, V_{\mathrm{ANISO}}[r(t)]|J_i'M_i'J_2'M_2'\rangle \right|^2,$$

$$S_{2,i2}' = \frac{\hbar^{-2}}{2} \frac{1}{(2J_i+1)(2J_2+1)} \sum_{\substack{J_f',M_i' \\ J_2',M_2' \\ M_f,M_2}} \mathrm{P.P.} \int_{-\infty}^{+\infty} \frac{\mathrm{d}\omega}{\omega_{J_fJ_2,J_i'J_2'} - \omega}$$

$$\times \left| \int_{-\infty}^{\infty} \mathrm{d}t\, \mathrm{e}^{i\omega t} \langle J_iM_iJ_2M_2|\, V_{\mathrm{ANISO}}[r(t)]|J_i'M_i'J_2'M_2'\rangle \right|^2; \tag{5}$$

$S_{2,f2}$ and $S_{2,f2}'$ are obtained by changing the subscript i by f. In these equations, V_{ANISO} means the anisotropic part of the intermolecular potential and P.P. the Cauchy principal part. This approach, which is based on a partial resummation of the V-infinite series through the *connected* terms[10] $S_2^{(C)} = S_{2,f2} + S_{2,i2} + S_{2,f2i2}^{(C)} + i(S_{2,f2}' - S_{2,i2}')$, avoids the cutoff procedure of the Anderson theory.[11]

For the description of the classical translational motion, this model takes into account the influence of the isotropic interactions V_{ISO} on the trajectory.[12] This description represents a significant improvement to the Anderson theory in which the trajectory is a straight line described with constant velocity, because it avoids the unphysical situation in which the colliding molecules interpenetrate, thus leading to infinite values of the transition probability.

We now restrict the formalism to the rotational and Λ-doubling transitions of the molecule OH in the electronic ground state $^2\Pi$. The ground electronic state of OH is a $^2\Pi$ state because of an unpaired electron. The component of spin angular momentum $S = 1/2$ along the internuclear axis ($\Sigma = \pm 1/2$) is coupled to the component of the electronic orbital angular momentum $L = 1$ along the same axis ($\Lambda = \pm 1$). The total electronic angular momentum projection is $\Omega = \Lambda + \Sigma$. The electronic ground state is an inverted $^2\Pi$ state with the $^2\Pi_{1/2}(F_2)$ levels at higher energy than the $^2\Pi_{3/2}(F_1)$ levels.[13] The coupling for this state is intermediate between Hund's cases (a) and (b). Moreover the $^2\Pi$ state and the upper $^2\Sigma$ state perturb one another, and the interaction between the rotational and electronic motions in the molecule produce Λ doubling for each $J(^2\Pi_{1/2,3/2})$. In the electronic $^2\Pi$ ground state of OH, the vibration rotation energy levels are adequately described by the wave functions $\tilde{\psi}_{J,\Omega,M}$, which are defined for a given vibrational v

state by[14]

$$\left.\begin{aligned}\tilde{\psi}_{J,3/2,M} &= A(J)\psi(^2\Pi_{1/2}) + B(J)\psi(^2\Pi_{3/2}),\\ \tilde{\psi}_{J,1/2,M} &= -A(J)\psi(^2\Pi_{1/2}) + B(J)\psi(^2\Pi_{3/2}),\end{aligned}\right\} \quad (6)$$

with

$$A(J) = \left(\frac{X-2+\lambda}{2X}\right)^{1/2}, \quad B(J) = \left(\frac{X+2-\lambda}{2X}\right)^{1/2}$$

and

$$X = \left[4\left(J+\frac{1}{2}\right)^2 + \lambda(\lambda-4)\right]^{1/2}, \quad \lambda \equiv A/B = -7.501.^{13}$$

These wave functions are linear combinations of the $\psi(^2\Pi_{1/2})$ and $\psi(^2\Pi_{3/2})$, which are the eigenfunctions corresponding to pure Hund's case (a). The effect of the Σ state is neglected in constructing Eq. (6). Consequently a molecule in the $^2\Pi_{3/2}$ state has a finite probability of being found in the $^2\Pi_{1/2}$ state and vice-versa. Using the results of Green and Zare[15] and of Chu,[16] the $\psi(^2\Pi_{1/2})$ and $\psi(^2\Pi_{3/2})$ wave functions may be decomposed approximately into the product of electronic $\Phi_{el}(^2\Pi_{|\Omega|})$ and rotational wave functions $\Phi_{(J,\Omega,M,\epsilon)}$ given by

$$\psi(^2\Pi_{|\Omega|}) \simeq \Phi_{el}(^2\Pi_{|\Omega|}) \cdot \Phi(J, \Omega, M, \epsilon), \quad (7)$$

with

$$\Phi(J, \Omega, M, \epsilon) = \frac{1}{\sqrt{2}}[\Phi(J, \Omega, M) + \epsilon\Phi(J, -\Omega, M)],$$

where the $\Phi(J, \Omega, M)$ are the symmetric top wave functions and $\epsilon = \pm 1$ is the state parity.

The rotational constant of OH is so large ($18.544\,cm^{-1}$)[13] that the rotational levels characterized by the quantum number J are widely spaced (Fig. 1) and the rotational spectrum lies in the far-infrared. The pure microwave spectrum is due to transitions between Λ-doublets within a particular rotational level and was first observed by Dousmanis *et al.*[1] For OH, the strong coupling between rotational and electronic motions of the radical leads to large Λ-doubling. Each Λ-type doubling transition is split by magnetic hyperfine coupling due to hydrogen (which has nuclear spin $I = 1/2$) into four components characterized by the total angular momentum $F = J + I$ obeying the selection rule $\Delta F = 0, \pm 1$. The two lines arising from the $\Delta F = 0$ transitions are the strongest and are generally the only ones observed. Neglecting the hyperfine structure, the energy of each component of a particular doublet in the $^2\Pi_{1/2}(F_2)$ or $^2\Pi_{3/2}(F_1)$ state

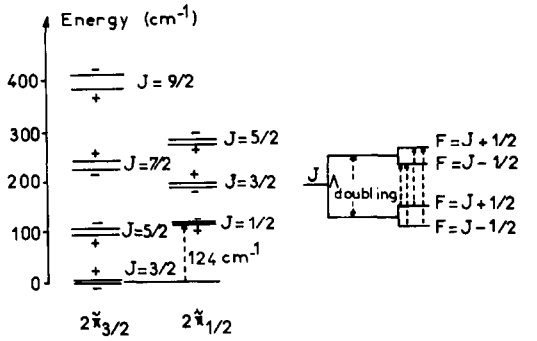

Fig. 1. Energy level diagram of OH showing rotational states of the lowest vibrational level for the $^2\Pi_{3/2}$ and $^2\Pi_{1/2}$ electronic states (not to scale). The hyperfine structure on the r.h.s. is indicated for the ground state Λ doubling.

is given by $F_{1,2}(J) \pm W/2$, with [13]

$$F_1(J) = B_v\left\{\left(J+\frac{1}{2}\right)^2 - 1 - \frac{1}{2}\left[4\left(J+\frac{1}{2}\right)^2 + Y(Y-4)\right]^{1/2}\right\} - D_v J^4,$$
$$F_2(J) = B_v\left\{\left(J+\frac{1}{2}\right)^2 - 1 + \frac{1}{2}\left[4\left(J+\frac{1}{2}\right)^2 + Y(Y-4)\right]^{1/2}\right\} - D_v (J+1)^4, \tag{8}$$

and[17]

$$W = \frac{q_\Lambda}{2}\left(J+\frac{1}{2}\right)\left[\left(2+\frac{A'}{B'}\right)\left(1 \pm \frac{2 - A/B}{X}\right) \pm \frac{4(J+3/2)(J-1/2)}{X}\right]; \tag{9}$$

X has been defined in Eq. (6). In Eq. (9), the upper and lower signs refer to the $^2\Pi_{1/2}$ and $^2\Pi_{3/2}$ states, respectively.

The numerical values of the rotational constants in the ground $^2\Pi$ state of OH are[13,17,18]

$$B_0 = 18.544\ \text{cm}^{-1},\ D_0 = 1.9071 \times 10^{-3}\ \text{cm}^{-1},\ A'/B' = -6.073,$$
$$q_\Lambda = 386.333 \times 10^{-4}\ \text{cm}^{-1}, \text{ and } Y = -7.41.$$

Some linewidth calculations in self-broadening or broadening by foreign gases were made previously.[5,8] However, the interaction potential was incompletely described and short range anisotropic forces were disregarded. Due to the large values of the dipolar and quadrupolar moments of OH (Table 1), the long-range electrostatic interactions between OH and linear molecules are expected to dominate broadening. In this work, in order to get a realistic description of the angle-dependent intermolecular potential, we have used both electrostatic interactions and atom–atom interactions,[9] which include an anisotropic short-ranged potential. Thus, the interaction potential V between OH and a foreign gas may be written as

$$V = V_A + V_E = \sum_{i,j}\left(\frac{d_{ij}}{r_{1i,2j}^{12}} - \frac{e_{ij}}{r_{1i,2j}^{6}}\right) + V_{\mu_1\mu_2} + V_{\mu_1 Q_2} + V_{\mu_2 Q_1} + V_{Q_1 Q_2}. \tag{10}$$

In Eq. (10), the indices i and j refer, respectively, to the ith atom of molecule 1 and the jth of molecule 2, $r_{1i,2j}$ is the distance between these two atoms, d_{ij} and e_{ij} are the atomic pair energy parameters and μ and Q are, respectively, the permanent dipolar and quadrupolar moments of the two molecules. Electrostatic contributions do not exist if the perturber is an atom. In the frame of Fig. 2, we obtain the following expression for the potential $V = V(R, \theta_1, \theta_2, \phi_1, \phi_2)$ in terms of the intermolecular distance r, of the intramolecular distances r_{1i} and r_{2j}, and of the spherical harmonics Y_l^m tied to each molecule:

$$V(r, \theta_1, \theta_2, \phi_1 - \phi_2) = 4\pi \sum_{l_1,l_2} \sum_{m=-\inf(l_1,l_2)}^{+\inf(l_1,l_2)} u_{l_1 l_2 m}(r)\, Y_{l_1}^m(\theta_1, \phi_1)\, Y_{l_2}^{-m}(\theta_2, \phi_2), \tag{11}$$

with

$$u_{000}(r) = \sum_{ij}\left\{\left[\frac{d_{ij}}{r^{12}} - \frac{e_{ij}}{r^6}\right] + (r_{1i}^2 + r_{2j}^2)\left[\frac{22 d_{ij}}{r^{14}} - \frac{5 e_{ij}}{r^8}\right] + \left(r_{1i}^4 + r_{2j}^4 + \frac{10}{3} r_{1i}^2 r_{2j}^2\right)\left[\frac{1001 d_{ij}}{5r^{16}} - \frac{14 e_{ij}}{r^{10}}\right]\right\},$$

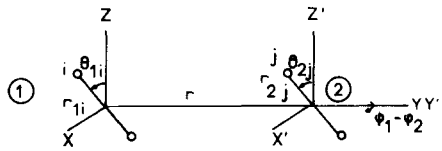

Fig. 2. Geometrical frame for interaction between two linear molecules.

Table 1. Physical parameters characterizing the intermolecular potentials for OH–Ar, OH–H_2, and OH–N_2.

	σ(Å) (a)	ε(°K) (a)	d_{ij} (b, f) (Kcal Å^{12}/mole)	e_{ij} (b,f) (Kcal Å^{6}/mole)	$\lvert r_{1i}\rvert$ ou $\lvert r_{2j}\rvert$ (b,c) (Å)	Q (d,e) (10^{-26} esu cm^2)	μ(d) (10^{-18}esu)	B_o (c) (cm^{-1})
OH | Ar	3.38	88.51	d_{HAr} = 253793 d_{OAr} = 488067	e_{HAr} = 280 e_{OAr} = 558	$\lvert r_{1H}\rvert$ = 0.9135 $\lvert r_{1O}\rvert$ = 0.0571 $\lvert r_{2Ar}\rvert$ = 0.	Q_{OH} = 1.81		B_o = 18.544 (OH)
OH | H2	3.18	52.37	d_{HH} = 26386 d_{OH} = 50559	e_{HH} = 53 e_{OH} = 106	$\lvert r_{2H}\rvert$ = 0.37075	Q_{H_2} = 0.66	μ_{OH} = 1.66	B_o = 60.8 (H_2)
OH | N_2	3.52	85.07	d_{HN} = 137908 d_{OH} = 265181	e_{HN} = 155 e_{ON} = 309	$\lvert r_{2N}\rvert$ = 0.5488	Q_{N_2} = - 1.52		B_o = 2.01 (N_2)

(a) Values determined from the potential curves of Figs. 4, 6, 7.

(b) From Ref. 19 and the usual combination rules.

(c) Ref. 13; (d) Ref. 16; (e) Ref. 20; (f) Ref. 21.

$$u_{100}(r)=\frac{1}{\sqrt{3}}\sum_{ij}\left\{r_{1i}\left[\frac{12d_{ij}}{r^{13}}-\frac{6e_{ij}}{r^{7}}\right]+\left(\frac{3}{5}r_{1i}^{3}+r_{1i}r_{2j}^{2}\right)\left[\frac{308d_{ij}}{r^{15}}-\frac{40e_{ij}}{r^{9}}\right]\right\},$$

$$u_{200}(r)=\frac{1}{\sqrt{5}}\sum_{ij}\left\{r_{1i}^{2}\left[\frac{56d_{ij}}{r^{14}}-\frac{16e_{ij}}{r^{8}}\right]+\left(r_{1i}^{4}+\frac{7}{3}r_{1i}^{2}r_{2j}^{2}\right)\left[\frac{704d_{ij}}{r^{16}}-\frac{400e_{ij}}{7r^{10}}\right]\right\},$$

$$u_{110}(r)=\sum_{ij}\left\{-r_{1i}r_{2j}\left[\frac{52d_{ij}}{r^{14}}-\frac{14e_{ij}}{r^{8}}\right]\right\}-\frac{2}{3}\frac{\mu_1\mu_2}{r^{3}},$$

$$u_{111}(r)=\sum_{ij}\left\{-r_{1i}r_{2j}\left[\frac{4d_{ij}}{r^{14}}-\frac{2e_{ij}}{r^{8}}\right]\right\}-\frac{\mu_1\mu_2}{3r^{3}},$$

$$u_{120}(r)=\frac{1}{\sqrt{(15)}}\sum_{ij}\left\{r_{1}r_{2j}^{2}\left[\frac{784d_{ij}}{r^{15}}-\frac{128e_{ij}}{r^{9}}\right]\right\}+\sqrt{\left(\frac{3}{5}\right)}\frac{\mu_1Q_2}{r^{4}},\tag{12}$$

$$u_{121}(r)=\frac{1}{\sqrt{5}}\sum_{ij}\left\{r_{1i}r_{2j}^{2}\left[\frac{56d_{ij}}{r^{15}}-\frac{16e_{ij}}{r^{9}}\right]\right\}+\frac{1}{\sqrt{5}}\frac{\mu_1Q_2}{r^{4}},$$

$$u_{210}(r)=\frac{1}{\sqrt{(15)}}\sum_{ij}\left\{-r_{1i}^{2}r_{2j}\left[\frac{784d_{ij}}{r^{15}}-\frac{128e_{ij}}{r^{9}}\right]\right\}-\sqrt{\left(\frac{3}{5}\right)}\frac{\mu_2Q_1}{r^{4}},$$

$$u_{211}(r)=\frac{1}{\sqrt{5}}\sum_{ij}\left\{-r_{1i}^{2}r_{2j}\left[\frac{56d_{ij}}{r^{15}}-\frac{16e_{ij}}{r^{9}}\right]\right\}-\frac{1}{\sqrt{5}}\frac{\mu_2Q_1}{r^{4}},$$

$$u_{220}(r)=\frac{1}{15}\sum_{ij}\left\{r_{1i}^{2}r_{2j}^{2}\left[\frac{12712d_{ij}}{r^{16}}-\frac{1328e_{ij}}{r^{10}}\right]\right\}+\frac{6Q_1Q_2}{5r^{5}},$$

$$u_{221}(r)=\frac{1}{5}\sum_{ij}\left\{r_{1i}^{2}r_{2j}^{2}\left[\frac{840d_{ij}}{r^{16}}-\frac{144e_{ij}}{r^{10}}\right]\right\}+\frac{4Q_1Q_2}{5r^{5}},$$

$$u_{222}(r)=\frac{1}{5}\sum_{ij}\left\{r_{1i}^{2}r_{2j}^{2}\left[\frac{56d_{ij}}{r^{16}}-\frac{16e_{ij}}{r^{10}}\right]\right\}+\frac{Q_1Q_2}{5r^{5}}.$$

For the atomic interaction between different kinds of atoms, the e_{ij} and d_{ij} may be deduced by means of the usual combination rules from the attractive parameters e_{kk} and the van der Waals radius $r_{\omega,kk}$ for related molecules with the same kinds of atoms, as obtained by Oobatake and Ooi[19] for a variety of molecules from second virial coefficients measurements, viz.

$$\left.\begin{aligned} r_{\omega,ij}&=\frac{1}{2}(r_{\omega,ii}+r_{\omega,jj}),\\ e_{ij}&=(e_{ii}e_{jj})^{1/2},\\ d_{ij}&=\frac{1}{2}e_{ij}(2r_{\omega,ij})^{6}. \end{aligned}\right\}\tag{13}$$

3. LINE-WIDTHS CALCULATION

We focus on molecular pairs for which experimental data are available. This is the case for OH perturbed by Ar for the $X^2\Pi_{3/2}J=5/2\leftarrow 3/2$ rotational transition[7] and also for OH perturbed by H_2 and N_2 in the $X^2\Pi_{3/2}$, $J=7/2$ and $J=11/2$ microwave transitions.[5,6] Although the broadening of OH–He was measured for these same transitions because this molecular pair is of major interest in connection with the atmospheric abundance of He, we have disregarded this problem because our formalism is not suitable to describe quantum effects tied to He.

The following numerical applications start from Eqs. (1)–(5) using the intermolecular potential of Eq. (10). The detailed expressions of the second-order differential $S_2(b)=S_{2,f2}+S_{2,i2}+S_{2,f2i2}^{(C)}$ and the $S_2^{(L)}(b)=S_{2,f2i2}^{(L)}$ are given in Appendix C of Ref. 9. The S_2' terms [Eq. (1)], which result from the non-commutative character of the intermolecular potential, were neglected since their contributions to line broadening were found to be negligible. Consequently, we put $\cos(S_{2,f2}'-S_{2,i2}')=1$. All calculations refer to room temperature. In order to reduce the computing

time, the calculations were performed for $\bar{v}$, which is a realistic simplification for the temperature of concern.

Due to the specific nature of the OH molecule, the dipolar absorption selection rule is $\Delta J = 0, \pm 1$; $\pm \rightarrow \mp$ (the + or − signs refer to the parity of the initial and final levels. In the ground state $v = 0$, $\Delta J = 0$ corresponds to the microwave absorption spectrum and $\Delta J = +1$ corresponds to the pure rotational absorption spectrum. Moreover, collision-induced transitions obey the selection rules $\Delta J = 0, \pm 1, \ldots, \pm l_1$, l_1 being the order of the spherical harmonics tied to the active molecule [here $l_1 = 1$ or 2, See Eqs. (11) and (12)] and $\Delta J_2 = 0, \pm 2, \ldots, \pm l_2$ when the perturbing molecule is a homonuclear diatomic molecule (here $l_2 = 2$). The parity rules tied to the $l_1 = 1$ and $l_1 = 2$ collisional transitions are $\pm \rightarrow \mp$ and $\pm \longrightarrow \pm$, respectively. The values of the Clebsch–Gordan coefficients are listed in Table 2 for the $^2\Pi_{1/2}$ and $^2\Pi_{3/2}$ electronic states for $l_1 = 1$ and 2. Because the OH rotational wave functions in the $^2\Pi$ state are linear combinations of pure Hund's case (a) rotational wave functions [$^2\Pi_{1/2}$ and $^2\Pi_{3/2}$, (Eq. (7)], we must consider not only induced transitions in the same state ($^2\tilde{\Pi}_{1/2} \rightarrow {}^2\tilde{\Pi}_{1/2}$, $^2\tilde{\Pi}_{3/2} \rightarrow {}^2\tilde{\Pi}_{3/2}$) but also induced transitions between different states ($^2\tilde{\Pi}_{1/2} \rightarrow {}^2\tilde{\Pi}_{3/2}$ and $^2\tilde{\Pi}_{3/2} \rightarrow {}^2\tilde{\Pi}_{1/2}$). Figure 3 summarizes this situation for the initial level $J_1 = 7/2$ in the $^2\tilde{\Pi}_{3/2}$ state.

We will now examine different molecular systems.

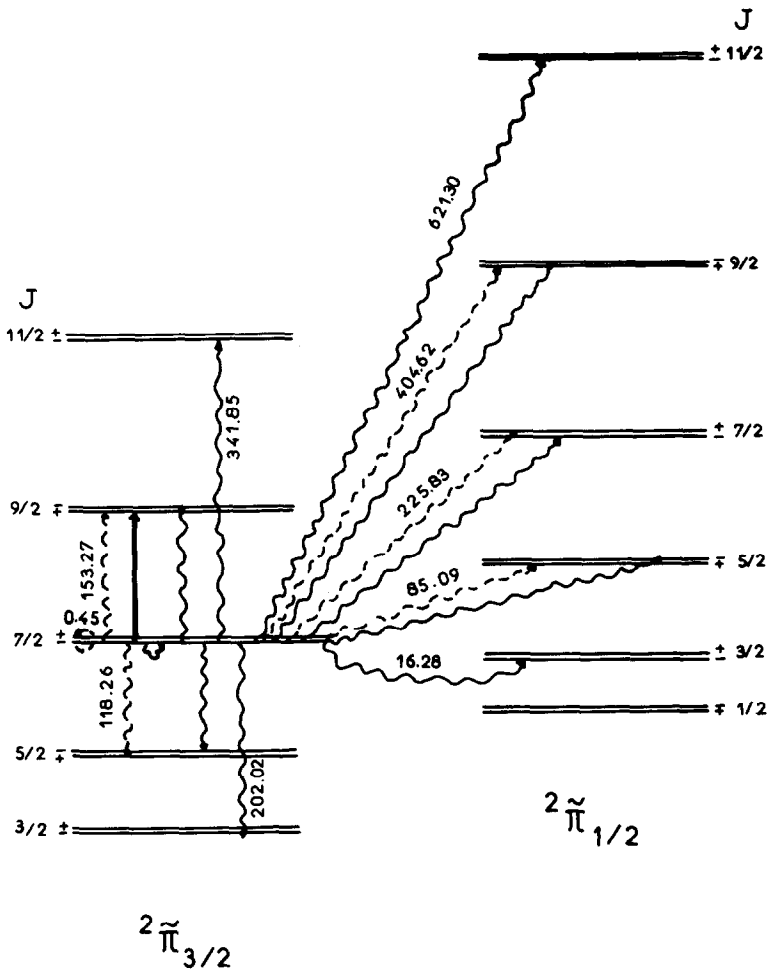

Fig. 3. Scheme of the collision induced transitions from the $^2\tilde{\Pi}_{3/2}$, $J_i = 7/2$ level. ⟶: optical transition; - - -: $\Delta J = 0, \pm 1$, $\pm \rightarrow \mp$ induced transitions; ⟿: $\Delta J = 0, \pm 1, \pm 2$, $\pm \rightarrow \pm$ induced transitions. The energies are in cm^{-1}.

Table 2. Clebsch–Gordan coefficients $C^{(l_1)}_{J,J',|\Omega|} \equiv C(J' l_1 J; |\Omega|, 0, |\Omega|)$ and the coefficients $A(J)$ and $B(J)$ appearing in Eq. (6) for the two $^2\tilde{\Pi}_{1/2}$ and $^2\tilde{\Pi}_{3/2}$ states.

J	A(J)	B(J)	J' = J - 1	J' = J	J' = J + 1	J' = J - 2	J' = J - 1	J' = J	J' = J + 1	J' = J + 2
			$C^{(1)}_{J,J',1/2}$			$C^{(2)}_{J,J',1/2}$				
1/2	0.0001	1.0000	0.0000	0.3333	0.6667	0.0000	0.0000	0.0000	0.4000	0.6000
3/2	0.1739	0.9848	0.3333	0.0667	0.6000	0.0000	0.2000	0.2000	0.0857	0.5143
5/2	0.2653	0.9642	0.4000	0.0286	0.5714	0.2000	0.0571	0.2286	0.0381	0.4762
7/2	0.3354	0.9421	0.4286	0.0159	0.5556	0.2571	0.0286	0.2381	0.0216	0.4545
9/2	0.3898	0.9209	0.4444	0.0101	0.5455	0.2857	0.0173	0.2424	0.0140	0.4406
11/2	0.4324	0.9017	0.4545	0.0070	0.5385	0.3030	0.0117	0.2448	0.0098	0.4308
13/2	0.4661	0.8847	0.4615	0.0051	0.5333	0.3147	0.0084	0.2462	0.0072	0.4235
15/2	0.4932	0.8699	0.4667	0.0039	0.5294	0.3231	0.0063	0.2471	0.0056	0.4180
17/2	0.5152	0.8570	0.4706	0.0031	0.5263	0.3294	0.0050	0.2477	0.0044	0.4135
19/2	0.5335	0.8458	0.4737	0.0025	0.5238	0.3344	0.0040	0.2481	0.0036	0.4099
21/2	0.5487	0.8360	0.4762	0.0021	0.5217	0.3383	0.0033	0.2484	0.0030	0.4070
23/2	0.5616	0.8274	0.4783	0.0017	0.5200	0.3416	0.0027	0.2487	0.0025	0.4044
25/2	0.5727	0.8198	0.4800	0.0015	0.5185	0.3443	0.0023	0.2489	0.0021	0.4023
			$C^{(1)}_{J,J',3/2}$			$C^{(2)}_{J,J',3/2}$				
3/2	0.1739	0.9848	0.0000	0.6000	0.4000	0.0000	0.0000	0.2000	0.5143	0.2857
5/2	0.2653	0.9642	0.2667	0.2571	0.4762	0.0000	0.3429	0.0143	0.2857	0.3571
7/2	0.3354	0.9421	0.3571	0.1429	0.5000	0.1429	0.2143	0.0857	0.1753	0.3818
9/2	0.3898	0.9209	0.4000	0.0909	0.5091	0.2143	0.1403	0.1364	0.1175	0.3916
11/2	0.4324	0.9017	0.4242	0.0629	0.5128	0.2545	0.0979	0.1680	0.0839	0.3956
13/2	0.4661	0.8847	0.4396	0.0462	0.5143	0.2797	0.0719	0.1885	0.0628	0.3971
15/2	0.4932	0.8699	0.4500	0.0353	0.5147	0.2967	0.0550	0.2022	0.0488	0.3973
17/2	0.5152	0.8570	0.4575	0.0279	0.5146	0.3088	0.0433	0.2119	0.0389	0.3970
19/2	0.5335	0.8458	0.4632	0.0226	0.5143	0.3179	0.0350	0.2190	0.0318	0.3964
21/2	0.5487	0.8360	0.4675	0.0186	0.5138	0.3248	0.0289	0.2242	0.0264	0.3957
23/2	0.5616	0.8274	0.4710	0.0157	0.5133	0.3303	0.0242	0.2283	0.0223	0.3949
25/2	0.5727	0.8198	0.4738	0.0133	0.5128	0.3348	0.0206	0.2314	0.0191	0.3941

OH–Ar

As the electrostatic interaction does not exist when OH is perturbed by a rare gas, a good description of the dispersion interaction is crucial. Figure 4 exhibits the radial part of the OH–Ar interaction energy. The anisotropic dispersion forces are essentially short-ranged so that the r^{-13}, r^{-14}, r^{-15}, and r^{-16} terms in the interaction potential [Eq. (12)] are expected to dominate broadening. Since the atom–atom development is not rapidly convergent, the neglected higher order terms may also contribute to the broadening.

The OH–Ar collision cross sections (σ) and half widths at half intensity [$\Delta\nu_{(1/2)}$] were calculated in the rotational spectrum and in the microwave spectrum for the $^2\tilde{\Pi}_{1/2}$ and $^2\tilde{\Pi}_{3/2}$ electronic states. The results are shown in Figs. 5(a) and 5(b). A comparison is also shown for the $^2\tilde{\Pi}_{3/2}$ $J = 3/2 \rightarrow 5/2$ transition with experimental data of Burrows *et al.*[7] (See Table 3). The theoretical value is in reasonable agreement with experiments. A similar calculation was performed in the pure Hund's case (a) by putting $A(J) = 0$ and $B(J) = 1$ in Eq. (6) and replacing $F_{1,2}(J)$ of Eq. (8) by[22]

$$F_{1,2}(J) = \left\{ \pm \frac{A}{2} + B_v[J(J+1) - \Omega^2] + \frac{B_v}{2} \right\}$$

$$(+ A/2 \text{ if } \Omega = 3/2 \text{ and } - A/2 \text{ if } \Omega = 1/2);$$

also W of Eq. (9) was replaced by

$$W = a(J + 1/2) \text{ if } \Omega = 1/2 \text{ or } W = b(J^2 - 1/4)(J + 3/2) \text{ if } \Omega = 3/2,$$

with $a = 0.316\,\text{cm}^{-1}$ and $b = 0.011\,\text{cm}^{-1}$.[17] We obtain $\Delta\nu_{(1/2)} = 39.7 \times 10^{-3}\,\text{cm}^{-1}\,\text{atm}^{-1}$ for the $J = 3/2 \rightarrow 5/2$, $^2\Pi_{3/2}$ line. This value is only 8% lower than the value calculated in the intermediate case. Thus, the transitions induced between the $^2\tilde{\Pi}_{3/2}$ and $^2\tilde{\Pi}_{1/2}$ states do not contribute significantly to broadening. This fact permits us to discuss the theoretical results further. To our knowledge, Ref. 7 constitutes the single datum relative to the broadening of OH by Ar. It would be very useful to obtain experimental information concerning the J dependence. Because OH is

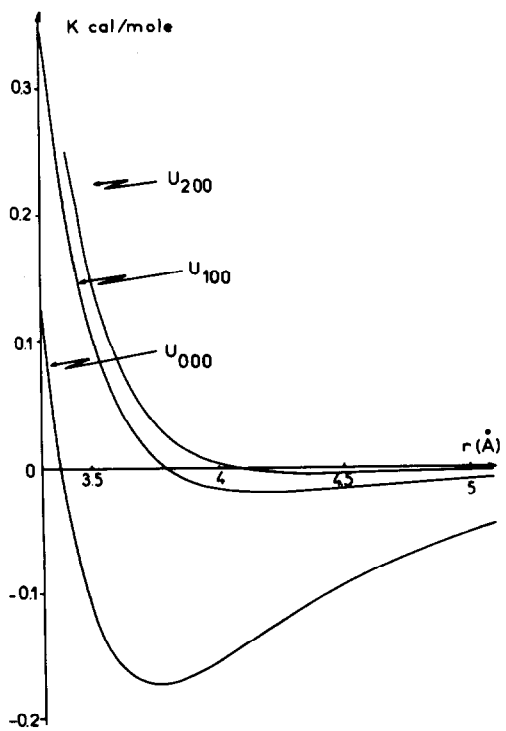

Fig. 4. The coefficients $u_{l_1 l_2 m}(r)$ in the spherical harmonics expansion for the interaction betrween OH and Ar.

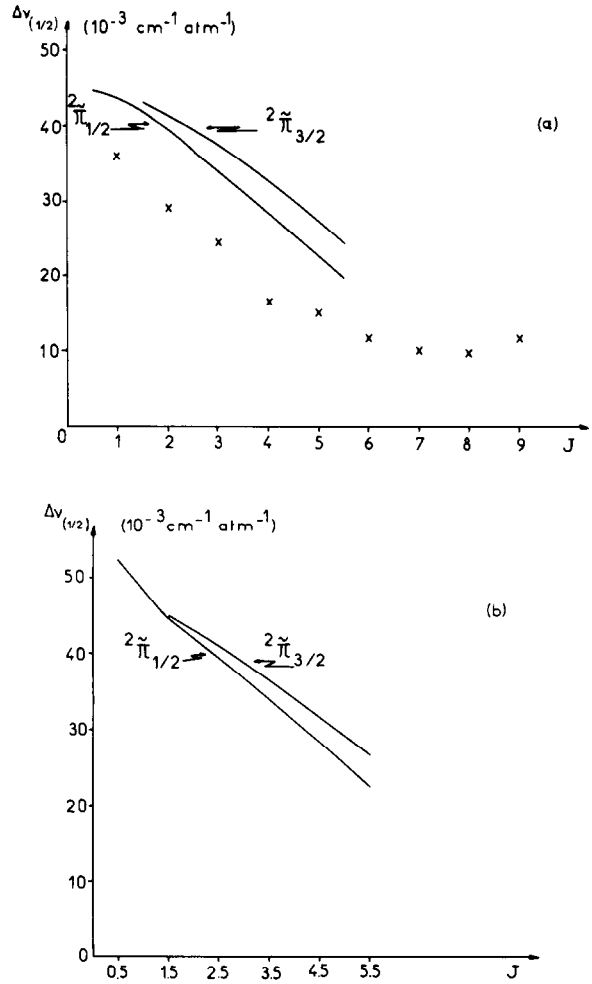

Fig. 5. Calculated half widths at half intensity for the OH-Ar lines; (a) x experimental data for pure rotational lines of HF–Ar in the same condition (x);[23] (b) microwave lines.

Table 3. Cross sections and half widths at half intensity for OH perturbed by various gases.

Colliding molecule	Transition	σ (Å^2)		$\Delta\nu$ (1/2) (10^{-3} cm^{-1} atm^{-1})	
		(a)	(b)	(a)	(b)
Ar	rotational ($J = \frac{3}{2} \rightarrow \frac{5}{2}$)	45.53	52.5	43.2	49
		(a)	(c)	(a)	(c)
H_2	($J = 7/2$) microwave	26.64	39-30	65.28	104
	($J = 11/2$)	22.82	22	55.91	58
N_2	($J = 7/2$) microwave	82	74-69	82.67	81
	($J = 11/2$)	47.28	79	47.64	86

(a) Values calculated in this work.

(b) Experimental values of Ref. 7.

(c) Experimental values of Refs. 5 and 6.

similar to HF insofar as the molecular parameters are concerned, a comparison seems possible between OH–Ar and HF–Ar broadenings. We have reported in Fig. 5(a) some experimental HF–Ar linewidths values.[23] The variations with J of the linewidths are very similar as expected. Thus, our theoretical results on OH–Ar seem credible both as to absolute magnitude of the widths and J-dependence. A slight differential broadening exists in OH, as was first observed in NO. This magnetic effect was discussed in a preceding paper.[24]

We now discuss the physical mechanisms causing broadening. Detailed calculations have shown that the predominant contribution comes from the repulsive part of the u_{100} term through the $\Delta J = \pm 1$ induced transitions (Fig. 4). The contribution coming from the u_{200} term is lowest because of the resonance properties in the collisional mechanisms (large value of the rotational constant B_0).[9] Since there is no possible resonance between the rotational states of OH and a rare gas atom, the linewidth decreases rapidly when J increases.

OH–H_2

The potential surfaces are presented in Figs. 6(a–c). For intermediate and long-range collisions, the u_{12} and u_{22} contributions of the atom–atom potential are negligible compared with the electrostatic contributions at the same angular dependence (see Figs. 6(b), (c)). This is due to the fact that the quadrupolar moments of both molecules are positive. Consequently, the dipole–quadrupole and quadrupole–quadrupole interactions behave like the short-ranged part of the atom–atom potential. Thus, the broadening of OH–H_2 lines, for impact parameters $b \lesssim 3.5$ Å, is caused by dipole–quadrupole and, to a lesser extent, by quadrupole–quadrupole interactions. On the other hand, for close collisions ($\sigma \lesssim b \lesssim 3.5$ Å), broadening is due to the atom–atom u_{100} and u_{200} contributions.

The microwave cross sections and linewidths of OH perturbed by H_2 were calculated for $J_i = 7/2$ and $J_i = 11/2$ in the $^2\Pi_{3/2}$ state. The results are shown in Table 3 and compared with experimental data of Bastard *et al.*[5,6]

Good agreement with experiments is obtained only for the $J_i = 11/2$ line; the experimentally observed variation of $\Delta\nu_{(1/2)}$, when passing from $J_i = 7/2$ to $J_i = 11/2$, is not at all understood. Indeed, when calculated in the pure Hund's case (a), the linewidths are $\Delta\nu_{(1/2)}[J_i = 7/2] = 61.18 \times 10^{-3}$ cm^{-1} atm^{-1} and $\Delta\nu_{(1/2)}[J_i = 11/2] = 53.05 \times 10^{-3}$ cm^{-1} atm^{-1}. These values are respectively, 6 and 5% lower than the corresponding values of Table 3. Hence, we may also compare OH–H_2 broadening with HF–H_2 broadening. In a recent paper, Mehrotra and Nair[25] report experimental observations and theoretical calculations for HF–H_2 linewidths in the first overtone band; for $J_i \geq 3$, the $\Delta\nu_{(1/2)}$ values decrease slowly as J_i increases. The same behaviour is obtained for OH–H_2 in our calculations, as will now be discussed.

Detailed calculations show that, for $J_i = 7/2$, the electrostatic and dispersion interactions with the same angular dependence contribute equally to broadening while, for $J_i = 11/2$, the dispersion interactions are predominant. Because the rotational constants of OH and H_2 are, respectively, 18.54 cm^{-1} and 60.8 cm^{-1} (see Table 2), resonances appear between the rotational states in both molecules for values of J_i obeying the approximate condition

$$J_i \sim \frac{B_2}{B_1}\frac{l_2}{l_1} J_{2\max}; \tag{14}$$

here, $J_{2\max}$ is the most populated level of the perturbing molecule at the given temperature ($J_{2\max} = 1$ at 300 K).[26] A resonance due to the u_{22} interaction appears for $J_i \sim 7/2$ and a resonance due to the strong u_{12} interaction appears for $J_i \sim 11/2$. While, at the same time, the contributions due to the u_{100} and u_{200} interactions decrease from $J_i = 7/2$ to $J_i = 11/2$, the addition of both of these effects results in a slow variation of the linewidth with J_i.

OH–N_2

The OH–N_2 potential surfaces are presented in Figs. 7(a)–(c) and are very different from those of OH–H_2 because of the negative value of the quadrupolar moment of N_2. Both the dipole–quadrupole and quadrupole–quadrupole interactions are now long-range, attractive forces and the consequence of the addition of the atom–atom contribution is occurrence of an important well in the energy curves. However, significant effects of the atom–atom potential

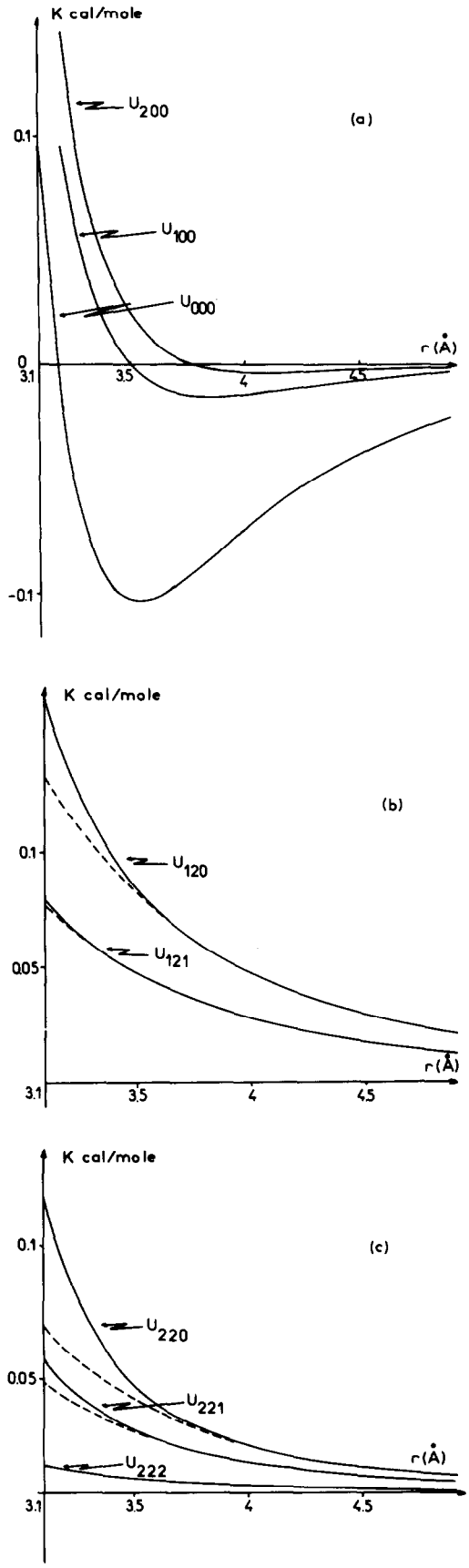

Fig. 6. The coefficients $u_{l_1 l_2 m}(r)$ for interactions between OH and H_2; ——; full potential; – – –: elec trostatic contribution only.

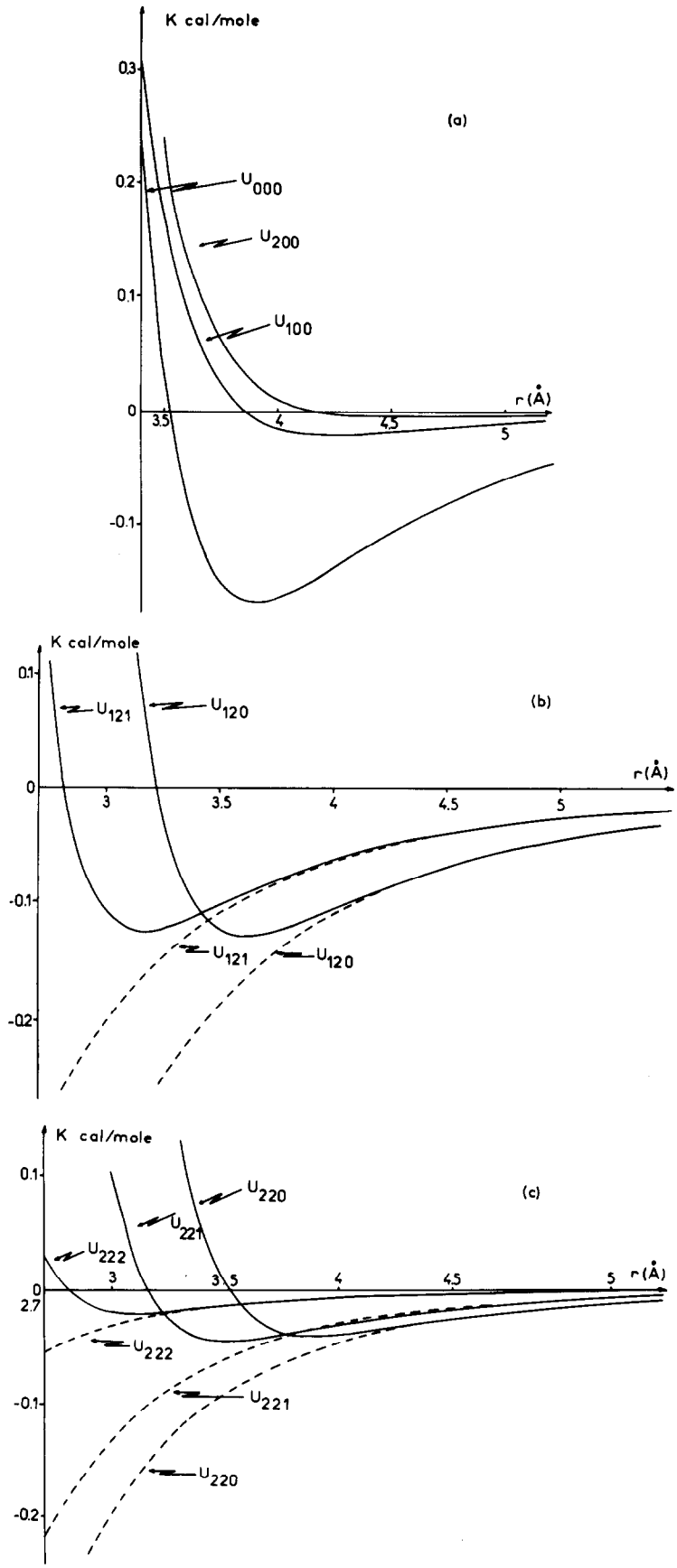

Fig. 7. The coefficients $u_{l_1 l_2 m}(r)$ for interactions between OH and N_2; ——; full potential; ----: electrostatic contribution only.

appear only for very strong collisions (impact parameters $< \sigma$), which are not dominant at room temperature. The broadening of OH–N_2 lines is thus due essentially to electrostatic dipole–quadrupole and quadrupole–quadrupole interactions.

The half-widths at half intensity $\Delta\nu_{(1/2)}$ of the microwave $^2\tilde{\Pi}_{3/2}$, $J_i = 7/2$ and $J_i = 11/2$ lines were calculated and compared with the experimental data of Refs. 5 and 6. Good agreement is now obtained between theory and experiment for $J_i = 7/2$, the theoretical value for $J_i = 11/2$ being half of the experimental value. As expected, the dominant contribution to OH–N_2 broadening was found to be due to electrostatic interactions, mainly dipole–quadrupole interaction. The rotational constant of N_2 is very small ($B_0 = 2.01\ cm^{-1}$) compared to that of OH, so that resonances due to electrostatic interactions would appear for $J_i \sim 1$ [see Eq. (14)]. Consequently, for $J_i \gg 1$, there is no resonance possible between the quantum states of OH and those of N_2. The variation with J_i of the half-width is then a rapid decrease, as was observed in similar cases (e.g. HF–N_2).[25]

Acknowledgements—The authors thank Prof. Charru and his collaborators for fruitful discussions and Prof. D. Robert for constant assistance with this work.

REFERENCES

1. G. C. Dousmanis, T. M. Sanders, Jr., and C. H. Townes, *Phys. Rev.* **100**, 1735 (1955).
2. G. Ehrenstein, C. H. Townes, and M. J. Stevenson, *Phys. Rev. Lett.* **3**, 40 (1959).
3. D. J. W. Kendall and T. A. Clark, *JQSRT* **21**, 511 (1979); many references are cited in this article.
4. R. Bustreel, J. L. Destombes, and C. Marliere, *Chem. Phys. Lett.* **42**, 154 (1976).
5. D. Bastard, A. Bretenoux, A. Charru, and F. Picherit, *JQSRT* **21**, 369 (1979).
6. D. Bastard, A. Bretenoux, A. Charru, and F. Picherit, *J. Phys. Lett.* **40**, L533 (1979).
7. J. P. Burrows, D. I. Cliff, P. B. Davies, G. W. Harris, B. A. Thrush, and J. P. T. Wilkinson, *Chem. Phys. Lett.* **65**, 197 (1979).
8. B. N. Lurie and J. M. Anderson, *Chem. Phys. Lett.* **36**, 614 (1975).
9. D. Robert and J. Bonamy, *J. Phys.* **40**, 923 (1979).
10. R. P. Leavitt and D. Korff, *J. Chem. Phys.* **74**, 2180 (1981).
11. P. W. Anderson, *Phys. Rev.* **76**, 647 (1949). C. J. Tsao and B. Curnutte, *JQSRT* **2**, 41 (1962).
12. J. Bonamy, L. Bonamy, and D. Robert, *J. Chem. Phys.* **67**, 4441 (1977).
13. G. Herzberg, *Spectra of Diatomic Molecules*, 2nd Edn. Van Nostrand, Princeton, New Jersey (Sept. 1966).
14. H. E. Radford, *Phys. Rev.* **122**, 114 (1961).
15. S. Green and R. N. Zare, *Chem. Phys.* **7**, 62 (1975).
16. S. I. Chu, *Astrophys. J.* **206**, 640 (1976).
17. C. H. Townes and A. L. Schawlow, *Microwave Spectroscopy*. McGraw-Hill, London (1955).
18. M. Mizushima, *Phys. Rev.* **5**, 143 (1972).
19. M. Oobatake and T. Ooi, *Prog. Theor. Phys.* **48**, 2132 (1972).
20. D. E. Stogryn and A. P. Stogryn, *Mol. Phys.* **11**, 371 (1966).
21. J. O. Hirschfelder, C. F. Curtiss, and R. B. Bird, *Molecular Theory of Gases and Liquids*. Wiley, New York (1967).
22. C. Alamichel, Thesis, Paris (1965).
23. T. A. Wiggins, N. G. Griffen, E. M. Arlin, and D. L. Kerstetter, *J. Molec. Spectrosc.* **36**, 77 (1970).
24. J. Bonamy, A. Khayar, and D. Robert, *Chem. Phys. Lett.* **83**, 539 (1981).
25. S. C. Mehrotra and K. P. R. Nair, *J. Chem. Phys.* **75**, 2479 (1981).
26. M. Giraud, D. Robert, and L. Galatry, *C. R. Acad. Sc.* **272**, 1252 (1971).
27. B. J. Robinson and R. X. McGee, *Ann. Rev. Astron. Astrophys.* **5**, 183 (1967).
28. S. I. Chu, M. Yoshimine, and B. Liu, *J. Chem. Phys.* **61**, 5389 (1974).